Journal of Biotechnology and Biodiversity

journal homepage: *https://sistemas.uft.edu.br/periodicos/index.php/JBB/index*

Antioxidant chondroitin sulfate extracted from Nile tilapia (*Oreochromis niloticus*) gill basis

Francisca Geny Marfim Fernandes[a], José Ariévilo Gurgel Rodrigues[a*], José Gabriel de Sousa Cândido[a], Ismael Nilo Lino de Queiroz[a], Johnny Peter Macedo Feitosa[a], Oscar Pacheco Passos Neto[a], Ianna Wivianne Fernandes de Araújo[a]

[a] Universidade Federal do Ceará, Brasil.
* Autor correspondente (arieviloengpesca@yahoo.com.br)

INFO

Keywords
waste
glycan
structural composition
oxidative stress

ABSTRACT

Gill of *Oreochromis niloticus* has glycosaminoglycans (GAGs), but their antioxidant potentials are unknown. This study partially examined gill (arches/bases) GAGs and analyzed as *in vitro* oxidative inhibitors. Tritured arches/bases were digested with papain and the GAGs characterized by electrophoreses (agarose/polyacrylamide) using known markers revealed in toluidine blue or stains-all; and their partially analyzed structure by infrared. Antioxidant potential of gill basis GAGs was examined by DPPH, total antioxidant capacity (TAC) and ferrous ion chelanging (FIC) assays comparing to BHT, ascorbic acid and EDTA, respectively. GAGs yield differed between parts (1.27 ± 0.03 *vs*. 0.45 ± 0.03%, P<0.05) and the techniques featured to a distinct charge composition between condroitin-6/4-sulfate (CS) chains (~40 kDa). *In vitro* antioxidant assays showed that basis GAGs potentially inhibited the DPPH radical similar to BHT (93.14 ± 0.38 *vs*. 95.68 ± 0.28% inhibition at 4 mg mL^{-1}, P>0.05), whereas for TAC and FIC revealed more reduced actions than the controls at the same amount of sample (<10/80% inhibition, respectively, P<0.05). The residual sugar composition of carboxylated and sulfated groups in CS structure suggested specific active sites on the reducing potencial in the initiation/propagation events. Therefore, CS from *O. niloticus* gill basis reveals to be a promissing antioxidant canditate.

Palavras-chaves
resíduo
glicana
composição estrutural
estresse oxidativo

RESUMO

Sulfato de condroitina antioxidante extraído de base branquial de tilápia do Nilo (Oreochromis niloticus)
A brânquia de *Oreochromis niloticus* possui glicosaminoglicanos (GAGs), porém são desconhecidos seus potenciais antioxidantes. Este estudo examinou GAGs parcialmente de brânquia e analisou como inibidores oxidativos *in vitro*. Arcos/bases triturados foram digeridos com papaína e caracterizados os GAGs por eletroforeses (agarose/poliacrilamida) usando marcadores conhecidos revelados em azul de toluidina ou "stains-all"; e, por infravemelho, sua estrutura analisada parcialmente. O potencial antioxidante foi examinado dos GAGs de base pelos ensaios DPPH, capacidade antioxidante total (CAT) e quelação do íon ferroso (CIF) comparando ao BHT, ácido ascórbico e EDTA, respectivamente. O rendimento de GAGs diferiu entre as partes (1,27 ± 0,03 *vs*. 0,45 ± 0,03%, P<0,05) e caracterizaram as técnicas para uma composição distinta na carga entre cadeias de sulfato-6/4 de condroitina (SC) (~40 kDa). Os ensaios antioxidantes *in vitro* mostraram que os GAGs de base inibiram potencialmente o radical DPPH equivalente ao BHT (inibição 93,14 ± 0,38 *vs*. 95,68 ± 0,28% em 4 mg mL^{-1}, P>0,05), enquanto ações mais reduzidas na mesma quantidade de amostra que os controles mostraram para CAT e QIF (inibições <10/80%, respectivamente; P<0,05). A composição de açúcar residual, na estrutura de SC em grupos carboxilados e sulfatados, sugeriu sítios ativos específicos sobre o potencial redutor nos eventos de iniciação/propagação. Portanto, SC de base branquial de *O. niloticus* revela-se um candidato antioxidante promissor.

© 2026 Journal of Biotechnology and Biodiversity
ISSN: 2179-4804
DOI: https://doi.org/10.20873/jbb.uft.cemaf.v14n3.21984

Creative Commons License. All the contents of this journal, except where otherwise noted, is licensed under a Creative Commons Attribution License.

INTRODUCTION

The aquaculture sector has technological capacity, farmed fish diversity and market opportunities (Moreira et al., 2001; Marques et al., 2023), but it generates non-edible by-products (*e.g.*, visceras, skins and heads) that affect the natural ecosystems at chemical and biological levels (Machado et al., 2020; Cooney et al., 2023). The eco-friendly transformation of these discards arises as sustaintable option to fish waste through bioprospecting of versatile polymers (*e.g.*, glycosaminoglycans-GAGs, peptides and collagens) (Cooney et al., 2023; Fernandes et al., 2025).

GAGs play physiological roles since fish mucus communities (Moreira et al., 2001; Koll et al., 2024) to speciation process (Pomin and Mourão, 2008). They have repetitive disaccharide units of a hexosamine (D-glucosamine or D-galactosamine) and uronic acid (D-glucuronic or L-iduronic) or galactose units. GAGs are linear and highly charged varying in sulfation pattern, glycosidic linkage and specific sugar sequence; being known heparin (HEP, highly charged), chondroitin sulfate (CS), dermatan sulfate (DS), hyaluronic acid (HA, nonsulfated), keratan sulfate and heparan sulfate (HS); but, those from terrestrial origin having viral risks (Pomin and Mourão, 2008; Badri et al., 2018). GAGs have grown over time (HEP, bovine/porcine lung and intestine; HA, microbial fermentation; and CS, bovine/porcine trachea and shark cartilage) as pharmaceutical products (Volpi, 2011; Badri et al., 2018). For CS (Figure 1), modifications naturally occur at other positions (mainly C-4/6-S) generating different structurally forms affecting or not their bioactivities (Garnjanagoonchorn et al., 2007; Couto et al., 2022; Li et al., 2022).

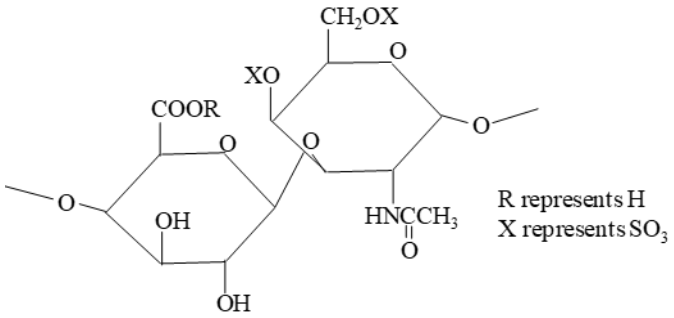

Figure 01 - Illustrative structure of CS based on Couto et al. (2022)

Reactive oxygen species arise from cellular metabolism that lead to oxidative stress of the living tissues causing free radicals-related diseases (*e.g.*, cancer, Alzheimer and atherosclerosis) and social impacts (Couto et al., 2022). Some natural sources have been described as novel antioxidant GAGs in comparison to synthetics which induce systhemic complications (Couto et al., 2022). For example, for sea snake (*Lapemis curtus*) skin and meat, Bai et al. (2018) suggested body-isolated GAGs as antioxidant candidates. Jridi et al. (2019) found a different structural composition between cuttlefish (*Sepia officinalis*) skin and muscle GAGs impacting for their *in vitro* antioxidant effects. Adult Nile tilapia (*Oreochromis niloticus*) viscera (Medeiros et al., 2021) and skin (Nascimento et al., 2021) revealed GAGs with intracellular antioxidant potential and non-toxic supplement for seminal cryopreservation of *Prochilodus brevis* fish, respectively. More recently, GAGs from hybrid fish "tambatinga" skin reduced *in vitro* oxidant reactions (Rodrigues et al., 2025). However, tilapia gill GAGs as antioxidant agents remain unexplored so far (Lima et al., 2025).

Gills of bony fish are cartilaginous structures playing respiratory function composed by arches, supported by two opposite bases into opercular cavity, and filaments, varying among species (Baldisserotto, 2002). They show roles related to exchange of gases/ions adaptated to ecological changes (Wasserman et al., 1972) similar to other aquatic animals (Regnault and Durand, 1998). Their matrices contain primarily collagen and mucopolysaccharides acting in animal physiology; but there is still scarce literature concerning production method and bioactivity of GAGs among cartilages found in different animal sources for biotechnological knowledge (Wasserman et al., 1972; Sundaresan et al., 2018; Li et al., 2022; Santiago et al., 2024).

The current study characterized arches *vs*. bases on their partial composition of CS by biochemical and structural approaches. Antioxidant potentials of Nile tilapia (*Oreochromis niloticus*) basis GAGs were also *in vitro* assessed, supporting new filleting waste valorization perspectives for tilapia GAGs isolation (Salles et al., 2017; Fernandes et al., 2025) from gills as cartilage by-products.

© 2026 Journal of Biotechnology and Biodiversity
ISSN: 2179-4804
DOI: https://doi.org/10.20873/jbb.uft.cemaf.v14n3.21984

MATERIAL AND METHODS

Farmed Nile tilapia gill samples

Initially, *in natura* gill samples were obtained from sex-reversed adult *O. niloticus* (n = 50) provided by the Aquaculture farm of Federal University of Ceará (FUC) (Figure 2A) (Marques et al., 2023). The fish were transported in ice (1:1 kg, biomass: ice ratio) with sialed isothermal boxes (Fernandes et al., 2025) and analyzed at the Marine Biochemical laboratory located at Aquaculture Biotechnology Center, Department of Fisheries Engineering, FUC. The specimens were registered in SisGen (National System for the Management of Genetic Heritage and Associated Traditional Knowledge) platform under code AA4816B and approved by the Animal Ethical Committee of the FUC (protocol nº 6974061020).

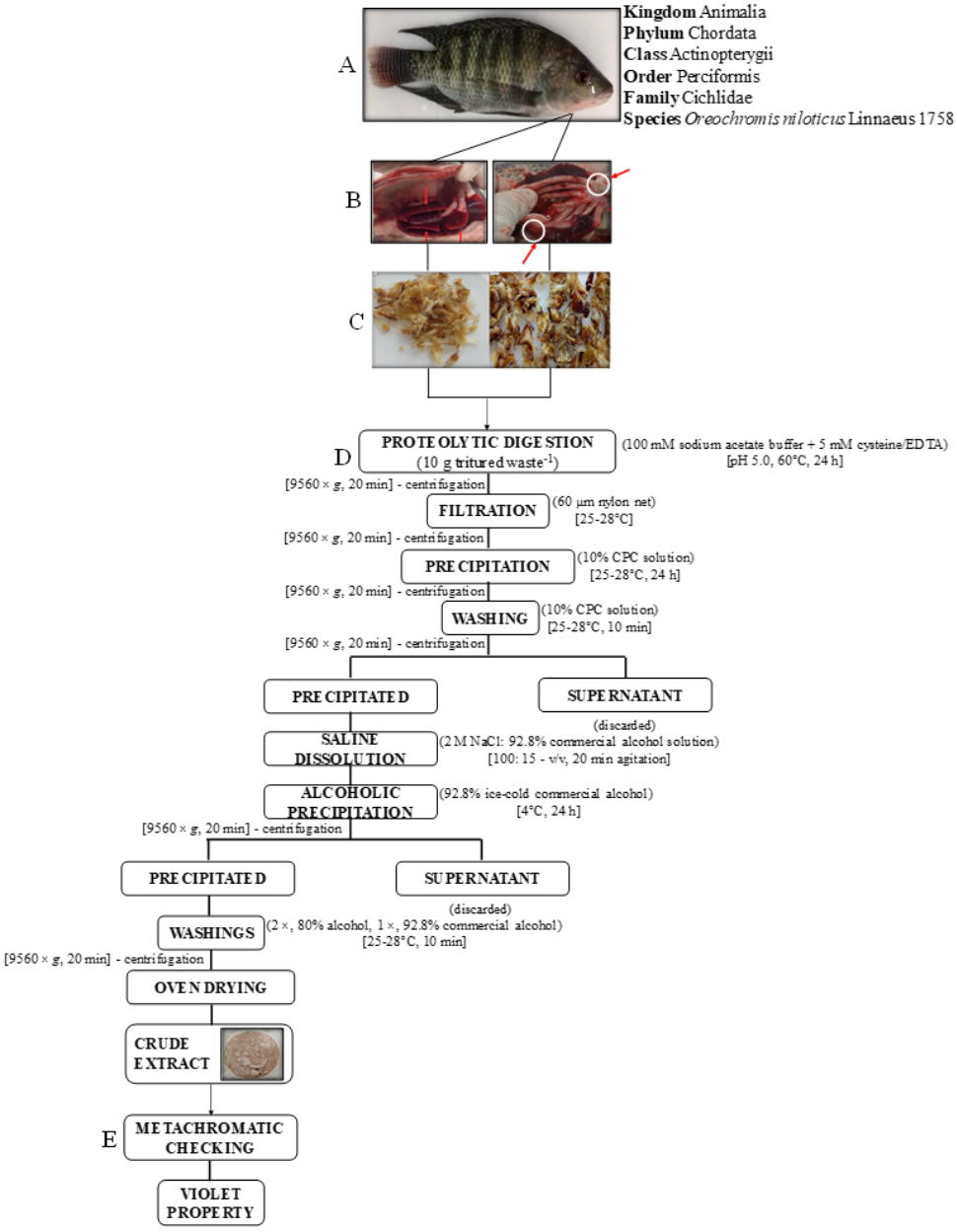

Figure 02 - Cultured Nile tilapia (A) showing its gill with arches (red sets, in left) sustained by opposite bases (white circle-red sets, in right) into opercular cavity (B) to obtain both dehydrated parts (C) for metachromatic sulfated GAGs extraction (D, E)

After that, fish were submitted to biometry (Fernandes et al., 2025) with average values 28.46 ± 2.51 cm and 409.14 ± 95.66 g from 52.93 kg fish biomass (Marques et al., 2023). Gill samples were manually removed from the opercular cavity with knife and, when necessary, flesh cutter to separate the gill from the animal head (Figure 2B) and, then, they were washed for cleaning of adherent

© 2026 Journal of Biotechnology and Biodiversity
ISSN: 2179-4804
DOI: https://doi.org/10.20873/jbb.uft.cemaf.v14n3.21984

particules, tissue blood and surface mucus before dehydratation (45°C, 24 h) (Figure 2C) (Santiago et al., 2024). Arches/bases were quantified from the whole gill; and both materials kept in separately closed recipients until tilapia GAGs obtaining (Lima et al., 2025).

GAGs extraction and metachromatic analysis

GAGs were separately extracted from fish gill (arches/bases) samples following protocol of Lima et al. (2025). Briefly (Figure 2D), both gill parts (10 g) in 100 mL of 100 mM sodium acetate buffer (pH 5.0) added with 5 mM EDTA/cysteine were treated with 15% papain for digestion at 60°C during 24 h in glass frask as reactor. The digested mixtures were filtered in 60 µm nylon net (25-28°C) and then centrifugated (9560 × *g*, 20 min) for save the supernatant in which the GAGs were, subsequently, precipitated with 10 mL of 10% cetylpyridinium chloride (CPC) solution (25-28°C) for 24 h. After that, mixtures centrifugated (9.560 × *g*, 20 min) yielded *pellets* containing GAGs that were washed with 100 mL of 0.05% CPC solution, dissolved for 20 min under mechanical stirring with 100 mL of a 2 M NaCl: 92.8% ethanol (100:15 ratio, v:v) solution, followed by addition of 100 mL of 92.8% ice-cold commercial ethanol for precipitation of GAGs (24 h, 4°C). The alcoholic precipitate was centrifugated (9.560 × *g*, 20 min), washed twice with 100 mL of 80% alcohol, and once with the same volume of 92.8% commercial alcohol. After centrifugation-sequential steps, both partially purified materials were dried (60°C, 24 h) yielding GAGs extracts as their percentages (% w w^{-1}, n = 3) from the initial first-matters (Santiago et al., 2024; Lima et al., 2025).

Metachromasy was analyzed following Fernandes et al. (2025)' residual comparative protocol. Initially, a solution of each crude GAGs sample was previously prepared and aliquots (9-27 µg, w v^{-1}) were *in vitro* tested with 1,9 dimethylmetilene (DMB) blue dye revealing colorimetric reaction by complex formed based on violet property to be specific for sulfated GAGs (Figure 2E) (Farndale et al., 1986) and photographic images recorded from a portable device with a resolution of 50 megapixels.

Partial identification by electrophoreses

Agarose gel electrophoresis (AGE) was used for characterizing of GAGs from both Nile tilapia gill (arches/bases) samples considerating charge density and homogeneity pattern (Dietrich and Dietrich, 1976). For this, test samples (~12 µg) were applied to a 0.5% agarose gel prepared in 0.05 M 1,3-acetate diaminopropane buffer at pH 9.0 and the run was carried out at constant voltage (100 V, 1 h). After procedure, the gel was immersed in a 0.1% *N*-cetyl-*N*,*N*,*N* trimethylammonium bromide solution for ~24 h to fix the GAGs and then it was dehydrated in oven with air circulation (55°C, ~6 h).

Polyacrylamide gel electrophoresis (PAGE) was conducted for evaluating the GAGs from both Nile tilapia gill (arches/basis) samples regarding their apparent molecular mass distribution and other contaminants. Similar to AGE technique, test samples (~12 µg) were applied to a 6% polyacrylamide gel using a system of 0.02 M Tris/HCl buffer at pH 8.6, of which a run was induced at 500 mA for 1 h (Santiago et al., 2024; Fernandes et al., 2025; Rodrigues et al., 2025).

Subsequently, both Nile tilapia gill (arches/bases) GAGs-presenting gels were stained with 0.1% toluidine blue or Stains-All cationic dye for 30 min and 24 h, respectively. Then, they were destained with a solution containing absolute ethanol, distilled water and acetic acid or using distilled water only (Fernandes et al., 2025). Chondroitin-6-sulfate (C-6-S, ~60 kDa), chondroitin-4-sulfate (C-4-S, ~40 kDa), sulfated dextran (DexS, ~8 kDa), dermatan sulfate (DS, ~40 kDa) and/or HEP (~15 kDa) were also employed as known markers for partial identification based on their mobilities on gels (Dietrich and Dietrich, 1976; Andrade et al., 2017). An integrated figure of both electrophoretic gels was contructed from the separatelly scaned preparations and images saved in Windows file.

Fourier Transform Infrared (FT-IR) spectroscopy

The structural composition of tilapia GAGs from gill (arches/bases) samples was investigated by FT-IR using a spectrometer (IRPrestige-21 Shimadzu, Japan). Each test sample (~10 mg) was pressed in potassium bromide (KBr) and the measurements were generated from pellets at a resolution of 4 cm^{-1}, with 64 scans min^{-1} at wavenumber 500-4000 cm^{-1}. The spectral value and the graphicals were assigned and represented using the Origin software version 8.0 as the Statistical Analysis Software (USA). The FT-IR spectra of both samples were separatelly saved in Windows file to construct the integrated figure.

In vitro antioxidant assays

The *in vitro* effect of tilapia GAGs from gill (bases) samples on the 1,1-diphenyl-2-picryl-hydrazil (DPPH) radical followed the study of Santiago et al. (2024). Different concentrations (0.125-4.0 mg mL^{-1}) of samples were added to the methanol solution of 75 M DPPH. After 30 min, absorbance (517 nm) was measured and all

© 2026 Journal of Biotechnology and Biodiversity
ISSN: 2179-4804
DOI: https://doi.org/10.20873/jbb.uft.cemaf.v14n3.21984

reactions were performed, in triplicates, and butylhydroxytoluene (BHT) was used as positive control. The DPPH scavenging effect was calculated using the following equation: scavenging activity (%) = $[A_0-(A-A_b)/A_0] \times 100$, where A_0 = DPPH without sample; A = sample + DPPH; and A_b= sample without DPPH.

The *in vitro* effect of tilapia GAGs from gill (bases) samples was analyzed by total antioxidant capacity (TAC) on the formation of the phosphomolybdate complex based on Santiago et al. (2024). For this, OnGAGs (0.125-4.0 mg mL^{-1}) from gill (bases) samples were added to a solution containing ammonium molybdate (4 mM), sulfuric acid (0.6 M), and sodium phosphate (28 mM), and were incubated at 95°C for 90 min. Absorbance (695 nm) was measured andall reactions were performed, in triplicate, and the ascorbic acid (AA, 200 g mL^{-1}) was considered a positive control as 100% TAC. Values were expressed as a percentage of TAC using the following formula: TAC (%) = $[(A_{sample}-A_{blank}) / (A_{ascorbic\ ac}-A_{blank})] \times 100$.

The *in vitro* effect of tilapia GAGs from gill (bases) samples on the ferrous ion chelating (FIC) followed the study of Santiago et al. (2024). Initially, different concentrations (0.125-4.0 mg mL^{-1}) of OnGAGs from gill (bases) samples were added to 0.1 mM ferrous sulfate ($FeSO_4$) and 0.25 mM ferrozine acid (3-(2-pyridyl)-5,6-diphenyl-1,2,4-triazine-p, p-disulfonic). The tubes were shaken (1 min), incubated (10 min) and the absorbance (562 nm) measured. All reactions were carrie out in triplicates and EDTA reagent was used as a positive control. Data were expressed as a percentage of chelating effect according to the following formula: FIC effect (%) = $[A_0-(A-A_b)/A_0] \times 100$, where A_0 = $FeSO_4$ + Ferrozine without sample; A = sample + $FeSO_4$ + Ferrozine; and A_b = sample without $FeSO_4$ + Ferrozine.

Statistical analyses

For experimental data (mean ± standard-deviation, n = 3) of extraction yield were adopted the *t*-Student' test between arches/bases. For amount of dehydrated tissues and *in vitro* antioxidant effects of GAGs were examined by the one-way univariate analysis of variance (ANOVA), followed by Tukey' test for gill arches and/or bases. P values < 0.05 were used statistically significant (Graph Pad Prism® software, version 5.01).

RESULTS AND DISCUSSION

Amount of dehydrated residual biomass

Whole gills of adult Nile tilapia were initially removed to obtain and compare their arches/bases (Figures 2). The dehydrated gill biomass yielded 0.65 ± 0.02% (w w^{-1}) of the fish volume *vs*. other wastes (skin, eyeball, intestine and gonad) from the same species already studied by Fernandes et al. (2025) comparatively analyzing among their relative rates. Regarding both gill parts, they comparatively differed (P < 0.05) between the analyzed samples, with arches as majority waste than bases (0.42 ± 0.01 *vs*. 0.23 ± 0.00%, w w^{-1}) from the dehydrated gill biomass, whose relative difference was 1.82-fold of the waste anatomy of *O. niloticus* (Figure 3) (Baldisserotto, 2002).

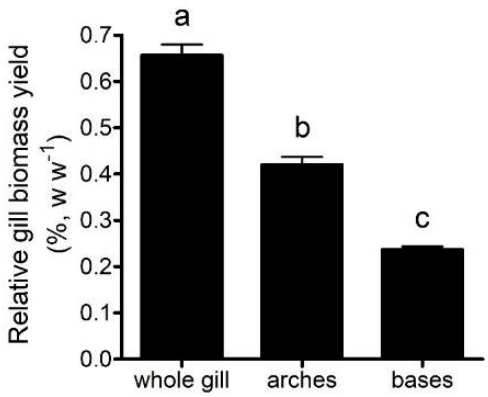

Figure 03 - Relative gill biomass, per dehydrated waste part, from cultured *O. niloticus*. Different letters on the bars revealing significant differences among gill wastes at level of 5% (ANOVA, Tukey' test, P < 0.05, n = 50)

Tilapia fish has a well-known technological chain having high consumption (Cooney et al., 2023), where heads (16.03%) (Moreira et al., 2001) making parts of filleting wastes showing composition comparable to that of the edible tissue (Machado et al., 2020). Gill integrates head as

© 2026 Journal of Biotechnology and Biodiversity
ISSN: 2179-4804
DOI: https://doi.org/10.20873/jbb.uft.cemaf.v14n3.21984

rejects that might be used for elaboration of silage and fish meal production (Moreira et al., 2001) transformating in useful products (Cooney et al., 2023; Fernandes et al., 2025). In this study, differentially dehydrated gill mass showed amount of parts that could be significantly impacted by anatomy of the filleted species (Moreira et al., 2001; Baldisserotto, 2002). The reduction of the constitution water from the fresh raw material could achieve comparatively higher GAGs yields than in *in natura* waste (Fernandes et al., 2025) suggesting a higher degree of security (Koll et al., 2024) for the production of safe bioactive polymers (Fernandes et al., 2025).

GAGs extraction yield

Tilapia gill (arches/bases) samples incubated with crude papain similar to experimental approach of Fernandes et al. (2025) combinating CPC and alcoholic precipitations resulted in different GAGs yields. The process confirmed good efficiency for obtaining of carbohydrates from cartilage by-products (Wasserman et al., 1972; Santiago et al., 2024; Lima et al., 2025), where the inedible parts yielded 1.27 ± 0.03 and 0.45 ± 0.03% (1.72% total yield, w w^{-1}) in crude GAGs, respectively ($P < 0.05$), from both dehydrated first-matters, but reaching 0.82% within the analyzed fish gill parts in available raw biomass (Figure 3), therefore, ~2.82-fold higher for arches-derived GAGs.

Gills in fishes have functional anology to lungs in vertebrates, but through a protective barrier of collagen and physiologically acting GAGs (Li et al., 2022) on microbial community (Koll et al., 2024), ionic/osmotic balance and immnunity of animal (Wasserman et al., 1972). In this study, dehydrated gill (arches/bases) samples from Nile tilapia indicated prospectives for GAGs as recently found by Lima et al. (2025) for whole gills (0.91 ± 0.03% w w^{-1}) using papain method. Other sources could also be compared, such as in whole gills of *C. maena* crab (7.52 ± 0.51 mg g^{-1}) by Regnault and Durand (1998); and in whole gills of *P. brevis* fish (1.54 ± 0.02%) by Santiago et al. (2024), but also in cartilages (tracheal, nasal and joint) of *Bubalus bubalis* buffalo (62.05 ± 0.5, 60.47 ± 1.19 and 60.76 ± 0.38 mg g^{-1}, respectively) (Sundaresan et al., 2018). Also, it still favorables than skins of *S. officinalis* (1.6%, Jridi et al., 2019), *O. niloticus* (0.1-0.22%, Salles et al., 2017; Nascimento et al., 2021; Fernandes et al., 2025), *P. brevis* (0.35 ± 0.03%, Fernandes et al., 2025) and hybrid "tambatinga" (0.37 ± 0.03%, Rodrigues et al., 2025); eyeballs (0.16 ± 0.03%), intestines (0.36 ± 0.10%) and gonads (0.40 ± 0.08%) of *O. niloticus* by Fernandes et al. (2025); but very low against muscles (8.6%, Jridi et al., 2019); and fins of skark (15.05 ± 0.73%), hyoids (27.37 ± 1.69%), ribs (9.05 ± 0.99%), sternums (9.05 ± 0.99%) and tracheas (14.72 ± 1.95%) of crocodile (Garnjanagoonchorn et al., 2007).

Vertebrate cartilages are higher sources in GAGs than fish ones (Li et al., 2022), except for cartilaginous fish due to their skeletal tissues rich in industrially-important anticoagulant/anti-inflammatory GAGs (Garnjanagoonchorn et al., 2007; Volpi, 2011; Badri et al., 2018). However, overfishing of elasmobranchs affects natural stocks (Li et al., 2022) and bony fish wastes arise as new market opportunities (Cooney et al., 2023; Fernandes et al., 2025), although with laborious accuracy and other related factors (Badri et al., 2018; Machado et al., 2020; Fernandes et al., 2025; Lima et al., 2025).

Combined biochemical identification of *O. niloticus* gill GAGs

The method of Farndale et al. (1986) complexity indicated, concentration-dependent, for a metachromatic sulfated GAGs composition in gill (arches/bases) matrix, as in GAGs isolated from other species' wastes (Fernandes et al., 2025; Lima et al., 2025) and animal sources (Regnault and Durand, 1998; Santiago et al., 2024; Rodrigues et al., 2025), since the violet property was found in both gill-integrating parts indirectaly indicating a cartilage matrix with a relatively different metachromatic GAGs concentration (Figure 4).

AGE analysis revealed homogeneous bands comigrating as standard CS (Figure 4D) (Lima et al., 2025), but differing in the charge density between both gill-parts GAGs by toluidin blue-treated gel from other wastes (Wasserman et al., 1972; Salles et al., 2017; Fernandes et al., 2025), which supported the metachromasy' results that revealed a discrepant colorimetric composition between samples (Figures 4A,C). The staining with the toluidin blue cationic dye also detected polymer complexed to buffer' diamine through of their sulfate radicals suggesting same spatial conformation (Dietrich and Dietrich, 1976).

These combined observations also reinforced to a different composition of sulfated GAGs in the gill matrix devoid of HA still verified by stains-all dye (Figure 4E) (Nascimento et al., 2021; Rodrigues et al, 2025), a clinically-important nonsulfated GAG (Badri et al., 2018). Other organisms revealed a complex mixture of cartilaginous tissue matrix' GAGs (Wasserman et al., 1972; Regnault and Durand, 1998; Pomin and Mourão, 2008) challenging industrial production for the high cost of separation and purity (Volpi, 2011; Badri et al., 2018; Cooney et al., 2023).

© 2026 Journal of Biotechnology and Biodiversity
ISSN: 2179-4804
DOI: https://doi.org/10.20873/jbb.uft.cemaf.v14n3.21984

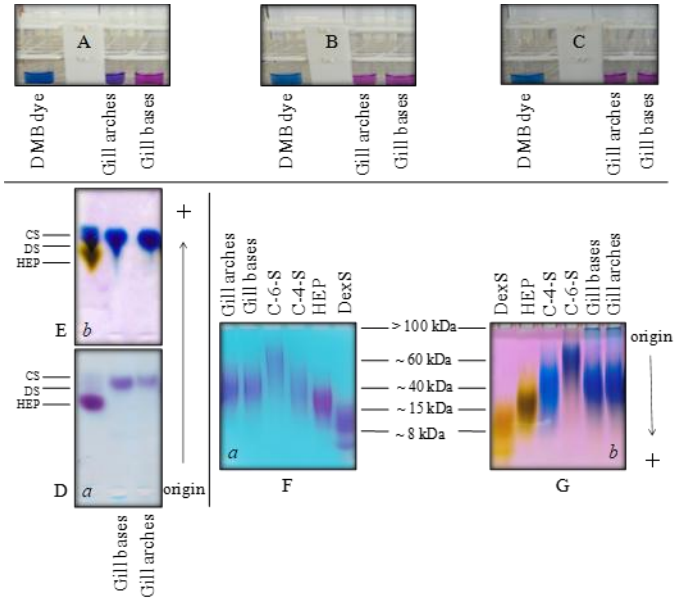

Figure 04 - Metachromasy assay (9-A, 18-B or 27 µg-C) and AGE (D, E) / PAGE (F, G) of GAGs extracted from *O. niloticus* gill arches/bases *vs*. known standards C-6/4-S (~60/40 kDa), DS (~40 kDa), DexS (~8 kDa) and/or HEP (~15 kDa) stained with 0.1% toluidin blue (*a*) or stains-all (*b*)

In PAGE system showed similar molecular distribution between preparations, by toluidin blue staining, with apparent mobility for CS GAGs of ~40 kDa size as respective standard (Figure 4F) (Andrade et al., 2017; Fernandes et al., 2025). Findings were also supported by AGE on the occurence of uniquely CS in tilapia gill (Li et al., 2022; Santiago et al., 2024), since the heterogeneous system regarding other blots (bright-blue), at the top of the gel, were attributed to protein-derived peptides by the protease action for GAGs extraction (Fernandes et al., 2025; Rodrigues et al., 2025) from the standard identities after stains-all staining (Figures 6F, G) and, at initial level, HA-free samples compared to mammalian GAGs (Andrade et al., 2017).

Structural composition of *O. niloticus* gill GAGs by FT-IR

FT-IR spectra of gill GAGs were practically identical concerning the functional groups present in both (arches/bases) samples, as illustrated in figure 5.

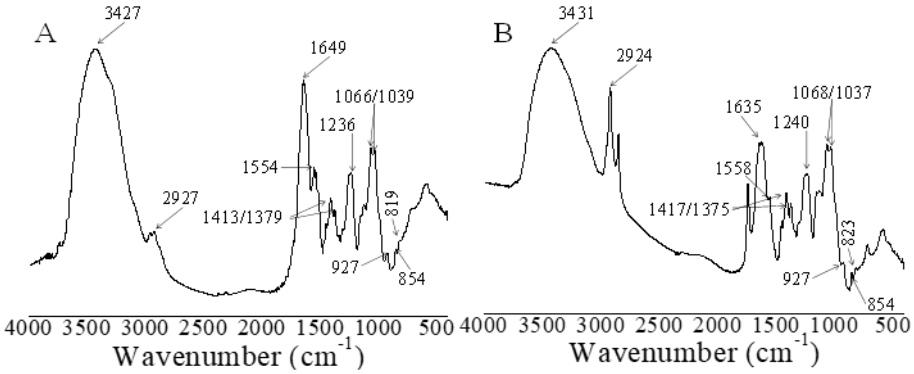

Figure 05 - FT-IR spectra of the Nile tilapia gill bases (A) / arches (B)-derived GAGs in KBr *pellets* at 500-4000 cm^{-1}

Spectral analysis showed GAGs chains (at 1200-900 cm^{-1}) with typical signals for CS at 3427-3431/2924-2927 (-OH/C-H), at 1236/1240 (-SO_3, total sulfation), at 1413-1417 (uronic acid), at 1635-1649 (C=O/N-H, amide I), at 1554-1558 (N-H, amide II) and at 1735-1379 (N-H, amide III) cm^{-1} (Jridi et al., 2019; Fernandes et al., 2025) characterizing its presence in the fish gill cartilaginous matrix (Santiago et al., 2024; Lima et al., 2025). The structural regularity between samples at level of specific sulfations (819-823/854 cm^{-1}), but with variable intensities at 1600-700 cm^{-1}

© 2026 Journal of Biotechnology and Biodiversity
ISSN: 2179-4804
DOI: https://doi.org/10.20873/jbb.uft.cemaf.v14n3.21984

[1] in the polymer, could explain those overall charge differences found in both parts (arches/bases) (Figures 5, 4D). This singularity of both C-6/4-S forms making part of the GAGs backbone (Figure 1) characterized the *O. niloticus* gill matrix in comparison to other sources (Garnjanagoonchorn et al., 2007; Sundaresan et al., 2018).

On a structural basis, the different GAGs composition found between both parts could perhaps support the biomechanical role of the gill during respiratory process (Figure 5A) (Baldisserotto, 2002) for the functionality of the arches (Wasserman et al., 1972; Li et al., 2022) based on glycan-conserved evidences to aquatic condition (Regnault and Durand, 1998; Pomin and Mourão, 2008; Li et al., 2022). The protease digestion applied in cultured *O. niloticus* gills as an eco-friendly criterium of industrial utilization (Badri et al., 2018; Fernandes et al., 2025) evidenced that more charged GAGs occured in minor amount in gill bases than those only dominating the arches anatomy (Wasserman et al., 1972; Lima et al., 2025), therefore, accessing different mucosal sites of the fish cartilage (Li et al., 2022) as previosuly observed by electrophoreses (Figure 4).

Collectivelly, both spectral profiles showed to be feasible CS structures for comparison with those of marine origin known of less complexity (Garnjanagoonchorn et al., 2007; Li et al., 2022), in the perspective of compare this hypothesis with various cartilage structures, when *O. niloticus* cultured in different conditions (Moreira et al., 2001).

In vitro antioxidant effects of *O. niloticus* gill GAGs by classical assays

GAGs from *O. niloticus* gill bases had consistent structural composition at level of charge density and purity (Figures 4D, 5A). So, they were chosen for their antioxidant effects by reducing concentration-dependent oxidative reactions (0.125-4.0 mg mL^{-1}) by all the *in vitro* tests, although showing differential roles (Figure 6).

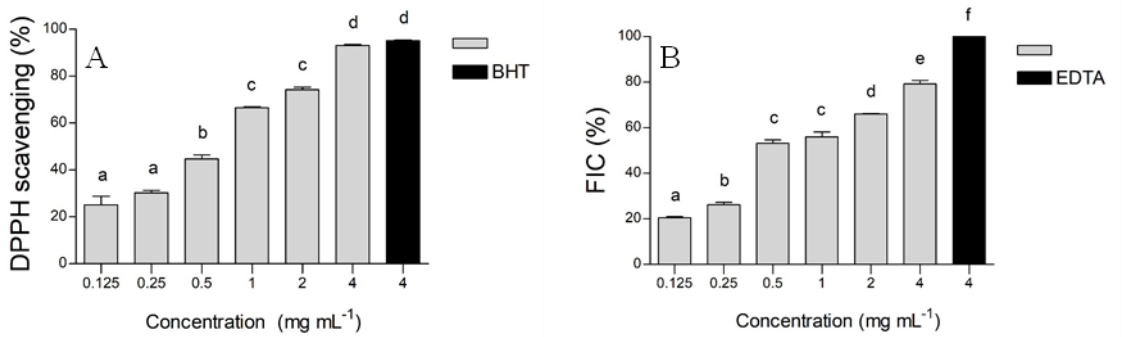

Figure 06 - Effects of *O. niloticus* GAGs from gill (bases) samples on DPPH radical (A) and FIC (B). Different letters among the bars indicate significative difference at level of 5% (ANOVA, followed by Tukey' test, $p < 0.05$, $n = 3$)

In the DPPH assay, GAGs were effective at >1 mg mL^{-1} ($P < 0.05$) and, potentially, at same level like BHT synthetic (93.14 ± 0.38 *vs*. 95.68 ± 0.28%, 4 mg mL^{-1}, $P > 0.05$) (Figure 6A); therefore, hydrogen donating substrate-like property (Bai et al., 2018; Jridi et al., 2019; Nascimento et al., 2021); Rodrigues et al., 2025). Still, they exerced good effect ($P < 0.05$) by FIC (~70-80% for 2/4 mg mL^{-1}) *vs*. EDTA action (97.12 ± 0.56%, 4 mg mL^{-1}) inhibiting biological peroxidation (Figure 6B) (Bai et al., 2018; Jridi et al., 2019; Medeiros et al., 2021; Nascimento et al., 2021; Rodrigues et al., 2025). Even TAC test, GAGs modestly acted on the formation of complex phosphomolybdates, inhibiting ($P < 0.05$) up to ~10% at 4 mg mL^{-1} *vs*. AA (100% inhibition, 0.12 mg mL^{-1}) (data not shown) (Bai et al., 2018; Nascimento et al., 2021; Rodrigues et al., 2025).

GAGs located on Nile tilapia gill bases matrix exibited preponderant active sites by DPPH radical-scavenging ability contrasting other glycans, but not excluding mechanisms to bind metallic compounds *in vitro* (Bai et al., 2018; Jridi et al., 2019; Nascimento et al., 2021; Rodrigues et al., 2025) possibly participating on the reaction chain of the gill physiology with unknown pathways (Wasserman et al., 1972; Regnault and Durand, 1998; Santiago et al., 2024) in response to culture conditions (Moreira et al., 2001), as for that CS from *O. niloticus* viscera devoid of cytotoxicity capable of reducing the intracellular oxidative radical level (Medeiros et al., 2021). The different composition of amide I/uronic acid residues between samples (Figure 5) could perharps justify the antioxidant potential by both initiation/propagation phases (Table 1), since the

© 2026 Journal of Biotechnology and Biodiversity
ISSN: 2179-4804
DOI: https://doi.org/10.20873/jbb.uft.cemaf.v14n3.21984

amount of attached sulfate groups would impact bioactivities (Pomin and Mourão, 2008; Sundaresan et al., 2018; Rodrigues et al., 2025), as sulfation at carbon 4 of galactosamine identified by FT-IR (Figures 1, 5) can be an essential substrate for the FIC ability eliminating reactive oxygen species that cause cell damage (Jridi et al., 2019; Medeiros et al., 2021); as in tilapia skin DS-cryopreserved semen (Nascimento et al., 2021) and in oxidant stress-related situations (Couto et al., 2022; Koll et al., 2024).

CONCLUSION

Gill of Nile tilapia has an anatomy that result in different raw biomass between arches/bases and availability in glycosaminoglycans located on its matrix. It showed be a valuable platform in regular chains of chondroitin-6/4-sulfate (~40 kDa size) dominating the arches while a more charged composition for gill bases in terms of amide I/uronic acid residues in the amount of sulfate groups that suggested as a factor for the prodution of animal antioxidants acting on both initiation/propagation phases comparing to commercial synthetics. Its chondroitin composition could opens new insights to better understanding other biological roles, as a promissing antioxidant canditate from cartilage by-products.

REFERENCES

Andrade JPS, Oliveira CP, Tovar AMF, Mourão PAS, Vilanova E. A color-code for glycosaminoglycans identification by means of polyacrylamide gel electrophoresis stained with the cationic carbocyanine dye Stains-All. **Electrophoresis**, v. 39, n. 4, p. 666-669, 2017. https://doi.org/10.1002/elps.201700391

Badri A, Williams A, Linhardt RJ, Koffas MA. The road to animal free glycosaminoglycan production: current efforts and bottlenecks. **Current Opinion in Biotechnology**, v. 53, p. 85-92, 2018. https://doi.org/10.1016/j.copbio.2017.12.018

Bai M, Han W, Zhao X, Wang Q, Gao Y, Deng S. Glycosaminoglycans from a sea snake (*Lapemis curtus*): Extraction, structural characterization and antioxidant activity. **Marine Drugs**, v. 16, n. 5, 170, 2018. https://doi.org/10.3390/md16050170

Baldisserotto B. Fisiologia de peixes aplicada à piscicultura. Santa Maria: Ed. UFSM, 212p. 2002.

Cooney R, Sousa DB, Fernandez-Rios AF, Mellett S, Rowane N, Morse AP et al. A circular economy framework for seafood waste valorisation to meet challenges and opportunities for intensive production and sustainability. **Journal of Cleaner Production**, v. 392, p. 136283, 2023. https://doi.org/10.1016/j.jclepro.2023.136283

Couto MR, Rodrigues, JL, Rodrigues LR. Heterologous production of chondroitin. **Biotechnology Reports**, v. 33, e00710, 2022. https://doi.org/10.1016/j.btre.2022.e00710

Dietrich CP, Dietrich SMC. Electrophoretic behaviour of acidic mucopolysaccharides in diamine buffers. **Analytical Biochemistry**, v. 70, n. 2, p. 645-647, 1976. https://doi.org/ 10.1016/0003-2697(76)90496-6

Farndale RW, Buttle DJ, Barrett AJ. Improved quantitation and discrimination of sulphated glycosaminoglycans by use of dimethylmethylene blue. **Biochimica et Biophysica Acta**, v. 883, n. 2, p. 173-177, 1986. https://doi.org/10.1016/0304-4165(86)90306-5

Fernandes FGM, Rodrigues JAG, Santiago LM, Queiroz INLQ, Feitosa JPM, Soares AS et al. Biochemical prospection of glycosaminoglycans in fish wastes aiming at circular economy. **Revista Brasileira de Engenharia de Pesca**, v. 16, n. 3, p. 18-33, 2025. https://doi.org/10.18817/repesca.v16i3.4116

Garnjanagoonchorn W, Wongekalaka L, Engkagulb A. Determination of chondroitin sulfate from different sources of cartilage. **Chemical Engineering and Processing**, v. 46, n. 5, p. 465-471, 2007. https://doi.org/10.1016/j.cep.2006.05.019

Koll R, Hauten E, Theilen J, Bang C, Bouchard M, Thiel R et al. Spatio-temporal plasticity of gill microbiota in estuarine fish. **Science of the Total Environment**, v. 957, 177505, 2024. https://doi.org/10.1016/j.scitotenv.2024.177505

Jridi M, Nasri R, Marzougui, Z, Abdelhedi O, Hamdi M, Nasri M. Characterization and assessment of antioxidant and antibacterial activities of sulfated polysaccharides extracted from cuttlefish skin and muscle. International **Journal of Biological Macromolecules**, v. 123, p. 1221-1228, 2019. https://doi.org/10.1016/j.ijbiomac.2018.11.170

Li W, Ura K, Takagi Y. Industrial application of fish cartilaginous tissues. **Current Research in Food Science**, v. 5, p. 698-709, 2022. https://doi.org/10.1016/j.crfs.2022.04.001

Lima ACN, Rodrigues JAG, Cavalcante LA, Feitosa JPM, Soares AS, Neto OPP. Combined fractionation for chondroitin sulfate-selective characterization from *Oreochromis niloticus* gills. Revista Brasileira de Engenharia de Pesca. v. 16, n. 3, p. 34-48, p. 2025. https://10.18817/repesca.v16i3.4073

Machado TM, Catapreta LC, Furlan EF, Neiva, CRP. Economia circular e resíduo de pescado. **Revista Brasileira de Ciências Ambientais**, v. 55, n. 4, p. 525-535, 2020. https://doi.org/10.5327/Z2176-947820200677

Marques DF, Neto OPP, Cordeiro W, Costa MP, Vanderley-Salmito CSB. Ultrafine bubble generator for oxygenation of Nile tilapia (*Oreochromis niloticus*) breeding tanks under recirculating water system. **Acta Veterinaria Brasilica**, v. 17, n. 2, p. 91-98, 2023. https://doi.org/10.21708/avb.2023.17.2.11242

Medeiros LHC, Vasconcelos BMF, Silva MB, Souza-Junior AA, Chavante SH, Andrade GPV. Chondroitin sulfate from fish waste exhibits strong intracellular antioxidant po-

© 2026 Journal of Biotechnology and Biodiversity
ISSN: 2179-4804
DOI: https://doi.org/10.20873/jbb.uft.cemaf.v14n3.21984

tential. **Brazilian Journal of Medical and Biological Research**, v. 54, n. 10, e10730, 2021. https://doi.org/10.1590/1414-431X2020e10730

Moreira HLM, Vargas L, Ribeiro RP, Zimmermann S. Fundamentos da moderna aqüicultura. Canoas: Ulbra, 200p. 2001.

Nascimento RP, Pereira VA, Almeida-Monteiro PS, Sales YS, Araújo IWF, Rodrigues JAG et al. Use of glycosaminoglycans from *Oreochromis niloticus* skin as an antioxidant supplement for milt cryopreservation of Brazilian bocachico. **Seminas: Ciências Agrárias**, v. 42, n. 5, p. 2959, 2021. https://doi.org/10.5433/1679-0359.2021v42n5p2959

Pomin VH, Mourão PAS. Structure, biology, evolution, and medical importance of sulfated fucans and galactans. **Glycobiology**, v. 18, n. 12, p. 1016-1027, 2008. https://doi.org/10.1093/glycob/cwn085

Regnault M, Durand F. Glycosaminglycans in gills of an intertidal grab (*Carcinus maenas*): changes in the gag population in response to prolonged air exposure. The **Journal of Experimental Zoology**, v. 281, n. 6, p. 554-564, 1998. https:// doi.org/10.1002/(SICI)1097-010X(19980815)281:6<554::AID-JEZ3>3.0.CO;2-M

Rodrigues JAG, Torres AB, Costa TO, Queiroz INL, Feitosa JPM, Soares AS et al. Antioxidant glycosaminoglycans extracted from the skin of "tambatinga", a hybrid fish. **Revista Brasileira de Engenharia de Pesca**, v. 16, n. 3, p. 49-64, 2025. https://doi.org/10.18817/repesca.v16i3.3711

Salles TC, Rodrigues JAG, Barcellos PG, Amaral GF, Araújo, IWF, Mourão PAS. Inhibition of thrombin generation by dermatan sulfate isolated from the skin of *Oreochromis niloticus*. **Brazilian Journal of Agricultural Sciences**, v. 12, n. 1, p. 98-104, 2017. https://doi.org/10.5039/agraria.v12i1a5412

Santiago LM, Rodrigues JAG, Queiroz INL, Costa TO, Feitosa JPM, Soares SA et al. *In vitro* evaluation of antioxidant action of chondroitin sulfate from the gills of *Prochilodus brevis*. **Revista Brasileira de Engenharia de Pesca**, v. 15, n. 1, p. 08-20, 2024. https://doi.org/10.18817/repesca.v15i1.3619

Sundaresan G, Abraham RJJ, Rao VA, Babu RN, Govind V, Meti MF. Established method of chondroitin sulphate extraction from buffalo (*Bubalus bubalis*) cartilages and its identification by FTIR. **Journal of Food Science and Technology**, v. 55, n. 9, p. 3439-3445, 2018. https://doi.org/10.1007/s13197-018-3253-4

Volpi N. Anti-inflammatory activity of chondroitin sulphate: new functions from an old natural macromolecule. **Inflammopharmacol**, v. 19, n. 6, p. 299-306, 2011. https://doi.org/10.1007/s10787-011-0098-0

Wasserman L, Ber A, Allalouf D. Acidic glycosaminoglycans composition of the gills of *Cyprinus carpio*. **Comparative Biochemistry and Physiology Part B**, v. 42, n. 4, p. 669-677, 1972. https://doi.org/10.1016/0305-0491(72)90328-8

© 2026 Journal of Biotechnology and Biodiversity
ISSN: 2179-4804
DOI: https://doi.org/10.20873/jbb.uft.cemaf.v14n3.21984